

FRACTURE TOUGHNESS DESIGN IN HORSE HOOF KERATIN

BY J. E. A. BERTRAM* AND J. M. GOSLINE

Department of Zoology, University of British Columbia, Vancouver, Canada

Accepted 17 April 1986

SUMMARY

An engineering fracture mechanics approach was applied to the analysis of the fracture resistance of equine hoof-wall. The relationship between fracture toughness and the morphological organization of the keratin hoof tissue was investigated. Fracture toughness was evaluated using the J-integral analysis method which employs the compact tension test geometry. Tensile tests were also conducted to evaluate the effect of the morphological organization on the stress-strain behaviour. Hoof-wall has greatest fracture resistance for cracks running proximally, parallel to the tubular component of the wall keratin. For fully hydrated material tested in this direction the mean critical J-integral value at failure was $1.19 \times 10^4 \text{ J m}^{-2}$. This was nearly three times greater than the value determined for the weakest orientation, in which the crack ran parallel to the material between the tubules. The lower fracture toughness of the intertubular material dominates the fracture behaviour of this tissue. The tubular components of the wall appear to reinforce against fracture along the weak plane and the entire wall organization provides the mechanical capability for limiting and controlling fracture in this tissue.

INTRODUCTION

The equine hoof-wall is an epidermal tissue which acts as an important component of the skeletal system. During locomotion, the hoof-wall is subjected to repeated high loads and abrasive interactions with the substrate. In a galloping thoroughbred, for example, the vertical force acting on each foot is equal to or greater than the animal's weight (about 9000 N). This load acts over a total contact time of approximately 0.1 s during each stride (Geary, 1975). This load must be transmitted to the ground through the distal contact surface of the hoof-wall, which has a total area of about 20 cm^2 . Thus, if the load is distributed uniformly over this area, the hoof-wall material experiences a stress of the order of 5 MPa. This level of stress is quite modest compared to the stresses required to break other components of the animal's skeleton, such as bone and tendon (Wainwright, Biggs, Currey & Gosline, 1982).

* Present address: Department of Anatomy, University of Chicago, Chicago, IL, USA.

Key words: keratin, hoof, fracture, toughness.

However, in the natural environment a horse would rarely encounter a substrate that allows a perfectly uniform distribution of stress over the contact surface. On uneven substrates, localized stresses may reach an order of magnitude greater than this. This extreme variability in loading means that the material from which the hoof-wall is constructed, i.e. keratin, may require mechanical properties which exceed those of other materials in the skeletal system.

Both man-made and natural structures break because the materials from which they are made fracture. Thus, a knowledge of the fracture properties of biological materials is essential to an understanding of the design of animal skeletons. Unfortunately, the process of fracture is quite complex and difficult to analyse, and, as a consequence, little is known about the fracture toughness of most biological materials. In fact, fracture toughness is often confused with strength, the maximum stress a material can sustain before it breaks, but strength alone is not a very useful parameter for describing how well a material or structure can resist breaking. For example, bone and wet wood have roughly the same tensile strength as glass (all at about 100 MPa), but obviously bone and wood are much more suitable materials from which to form the skeletons of animals and trees. If a piece of glass is hit with a hammer it shatters, whereas a similar impact on a piece of bone or wood may leave it dented, but not broken. This difference exists because fracture results from the uncontrolled growth of a pre-existing crack or flaw, a process that requires the creation of new surfaces, and crack growth is determined in large part by the amount of energy required to create these new surfaces. Thus, the energy required to create fracture surfaces, known as the work of fracture, is the most appropriate parameter for describing fracture toughness.

In this study we show that horse hoof keratin is one of the toughest biomaterials known, and that the organization of the keratin in the hoof-wall produces a tissue with integrated fracture toughness properties. This organization provides a material extremely well matched to its unique functional role.

Keratin is a fibre-reinforced composite material, formed from long, slender α -helical protein fibres embedded in an amorphous protein matrix (Fraser & MacRae, 1980). The cells that synthesize keratin die in the final stages of differentiation, when inter- and intramolecular disulphide crosslinks are established between the fibres and the matrix. It is this extensive molecular crosslinking that produces the stable composite. The mature keratin cells are flattened, elliptical discs (Wilkens, 1964), in which the α -helical fibres are oriented parallel to the long axis of the cells.

In the intact hoof this molecular composite is arranged in a complex pattern. Approximately half of the hoof-wall consists of cylindrical structures, called tubules, that run the length of the wall, parallel with the external surface of the hoof (Fig. 1). The axes of the cells and the fibres they contain are arranged in a steep spiral around the axes of the tubules. The intertubular portion of the wall keratin is composed of the same disc-shaped cells, but with cell axes and intracellular fibre orientations that cross the tubule axes. To date, it has not been possible adequately to explain the functional significance of this morphology in terms of stiffness or strength (Nickel,

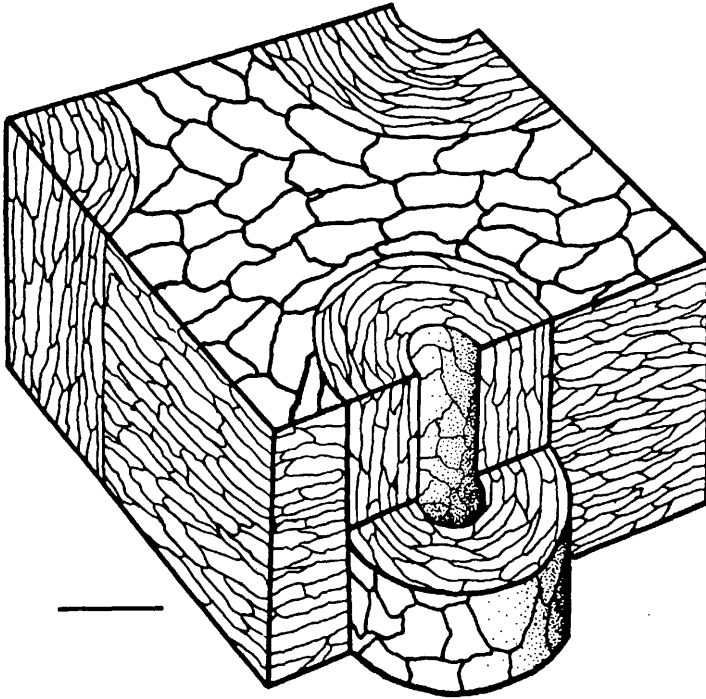


Fig. 1. Diagram of a small section of hoof-wall showing tubules, intertubular material and cellular organization. Top of drawing is proximal and view is looking from the outer portion of wall towards the inner portion. Scale bar, 100 μm .

1938; Dinger, Goodwin & Leffel, 1973; Leach, 1980). However, in this study we find a strong correlation between the keratin fibre organization and fracture toughness. This suggests that the hoof-wall morphology plays an important role in the ability of the hoof to resist and control fracture.

MATERIALS AND METHODS

The equine hoof-wall is part of the exterior epidermal hoof capsule. The wall proper covers the anterior, medial and lateral aspects of the equine foot. It is the load-carrying portion of the hoof and the major structural contact with the substrate (Leach, 1980; Parker, 1973; Sack & Habel, 1977). It is composed of three distinct layers. The most extensive, the *stratum medium*, has been studied in this investigation. The *stratum medium* is produced at the proximal border of the wall

(Fig. 2, *B*) and grows distally until it is worn off at the ground contact surface (Fig. 2, *C*).

The toe region of the hoof-wall of freshly killed, adult horses was sectioned by cutting parallel vertical strips with an industrial band saw. These strips were then cut into rough blocks. The blocks were machined to the appropriate dimensions for either tensile tests (0.6 mm thick, 4 mm wide, 2.5 cm long) or compact tension tests (CT) (1.0 cm total width, 1.0 cm height, 3 mm thickness) of fracture toughness. During the shaping, the blocks were kept fully saturated and cooled with distilled water. The blocks were cut to the appropriate thickness using a Micromet metallurgical saw, under a continuous flow of water. The precut notches of the CT specimens were cut with a single-edged razor blade mounted in a cutting jig. This procedure produced a sharp notch of reliable orientation.

The CT test specimen is a stout block of material with a deep notch cut into one side (Fig. 3) and loaded through pins which pass through the specimen on either side of the notch. This test geometry is commonly employed in the analysis of extremely tough engineering materials because it produces an intense stress concentration at the notch tip which drives crack growth in even the toughest materials. It also works well when the absolute dimensions of the test specimens are limited. It is designed to

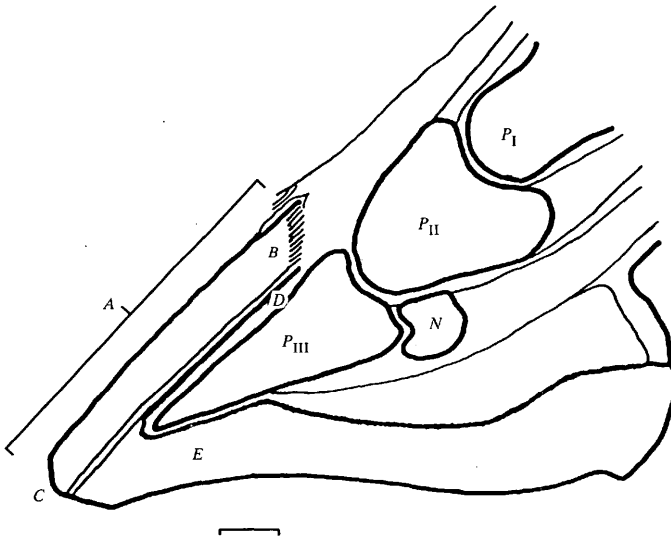


Fig. 2. Sagittal section of the equine foot showing the relationship of the hoof-wall to the other structures of the foot. *A*, hoof wall; *B*, generative portion of wall; *C*, distal contact surface; *D*, dermis; *E*, sole; *P*_I, *P*_{II}, *P*_{III}, phalanges of limb; *N*, navicular bone (distal sesamoid). Scale bar, 2 cm.

produce plane strain conditions during the fracture test, while using a minimum amount of test material. Plane strain occurs when all portions of the material in the plane of the precut notch are subject to the same strain. This situation is opposed to that of plane stress which occurs when the specimen does not possess adequate thickness. In the plane stress condition, lateral deformation near the surfaces of the specimen can allow stress equalization. The J-integral analysis assumes plane strain conditions. The size of specimen used in this study was the largest possible which would ensure that only *stratum medium* was included in the specimen. Although smaller in overall dimensions than recommended, the relative specimen dimensions were maintained consistent with those suggested for plane strain fracture analysis of metals (ASTM standard E-399-80), the only materials for which these standards have been developed.

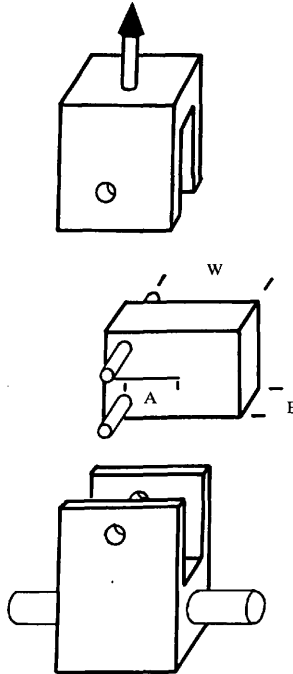


Fig. 3. Compact tension fracture test (CT) specimen and exploded view of loading clevis. B, full width of specimen; W, full ligament length measured from centre of loading pins to edge of specimen; A, notch length measured from centre of loading pins to end of precut notch. Lower clevis is secured to test chamber and test machine moving cross-head. Upper clevis is attached to 500 kg maximum force transducer.

To evaluate the role of morphology in the fracture properties, we constructed four different types of CT test samples with the notch cut at different orientations to the tubular and intertubular material. These four sample types are illustrated in Fig. 4. In orientation 1 the notch was cut parallel to the tubular axis, and therefore the notch would run in a proximal direction in the hoof-wall. Orientation 3 consisted of those samples in which the notch was cut normal to the tubular axis. The orientation of the intertubular material is more variable than that of the tubules. It was also difficult to determine exactly the orientation of the intertubular material prior to cutting the CT specimen. For these reasons the intertubular orientation is given as a mean in Table 3. The samples used for orientations 2 and 4 were cut so that the intertubular material was oriented either as steeply (mean angle 75.5°) or as shallowly (mean angle 14.1°) as possible to the notch direction.

Tensile testing

Tensile tests were conducted using an Instron Model 1122 tensile testing machine with a 500-kg load cell and extension rate of 5 mm min^{-1} . The tensile samples were tested in air, immediately after removal from water. All tests were finished within 2 min, and it is assumed that this was too short a time to alter the hydration level of the specimens. The samples were clamped at both ends using pneumatic sample grips. In order to eliminate end-effects due to sample gripping, specimen strain was measured by following the movement of surface fiducial marks placed well away from

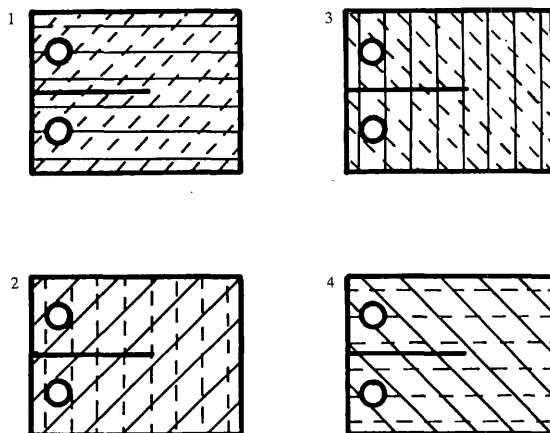


Fig. 4. Diagram of the relationship between the precut notch of the CT specimen and tubular and intertubular material for the four sample orientations used. Note that orientations 1 and 2 or 3 and 4 could be cut from the same sample by altering the direction of the notch. Tubular material orientation is designated by solid lines, intertubular orientation by dashed lines.

the test sample grip, using a video dimension analyser (Model 303, Instruments for Physiology & Medicine, La Jolla, CA).

Fracture testing

Fracture tests were carried out after the samples had become fully hydrated (5 or more days in water), and the tests were conducted with the specimens immersed in water. The samples were loaded using pins passing through holes on either side of the precut notch. The pins were attached to clevis mounts, which connected the specimen to the testing machine (Fig. 3). The test consists of pulling the load pins apart, perpendicular to the notch, creating a stress concentration near the notch tip. The loading clevis was built to contain two hinge axes which allowed each specimen individually to align with the direction of applied force during the test.

These tests produced a record of force (P) and extension (q) (Fig. 5A). The force/extension curve for CT specimens contained an initial linear portion of maximum stiffness. At higher load values the curve would deflect from this linear pattern and the apparent stiffness would decrease. It is believed that this change in slope indicates plastic deformation and stable crack growth at the crack tip (Wright & Hayes, 1977). The decrease in stiffness continued until the maximum load level was achieved (P_{max}). Extensive crack growth was associated with this point. In order to define a critical failure point for the test specimens, the maximum sustainable load (P_q) was determined as the load value of the test record given by the intersection of a 5% deviation from the initial linear portion of the test record, in accordance with the recommended procedure (see Fig. 5A; Landes & Begley, 1972).

The mechanical test records were digitized, and the force/extension curve was integrated at standardized intervals of load pin extension to determine the energy (U) which entered the specimen. The analysis of fracture behaviour in a material depends on accurately knowing the length of the crack that grows from the precut notch. Because the crack can be expected to grow to some extent prior to the critical failure point, it is important to monitor crack length continuously. A complex fibre composite, such as hoof-wall, makes visual measurement of crack growth difficult. An alternative to visual measurement, used successfully in the analysis of artificial composites (Gaggar & Broutman, 1975) and bone (Wright & Hayes, 1977), is compliance calibration. The compliance technique involves the determination of the compliance (i.e. the reciprocal of the apparent stiffness) of samples with *known notch length* (A) to width (W) ratios (Fig. 3). Compliance was calculated as

$$C = \frac{q}{P} \times B,$$

where q is load pin displacement, P is load and B is specimen width. A regression analysis was then performed to determine the mathematical relationship between crack length and compliance. This relationship is the compliance calibration. Since the compliance of the specimen is measured from force (P) and extension (q), this value can be taken from the test record for any point during the course of the test. An estimated crack length, termed the *apparent crack length* (a), can then be calculated

from the compliance calibration relationship. The lower case 'a' denotes the calculated *crack* length. This is derived from an analysis of specimens with known *notch* length, denoted with an upper case 'A'.

Fracture toughness was evaluated using the J-integral method (Rice, 1968), a technique which has proved useful with materials which show a considerable degree

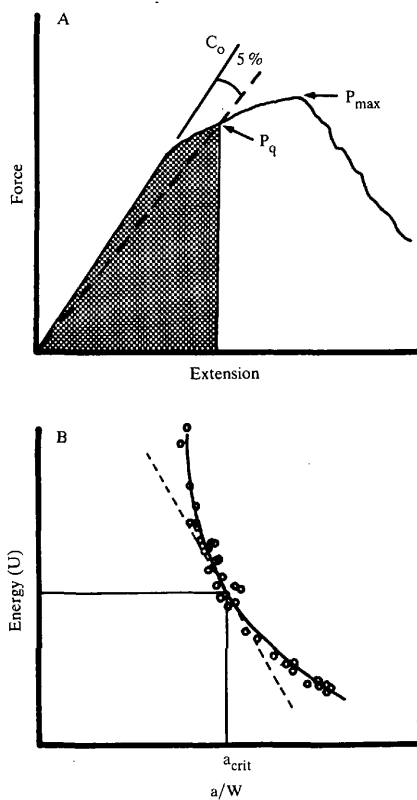


Fig. 5. (A) Analysis of compact tension fracture (CT) test record. Failure force and extension (P_q) are determined as the point at which a line from the origin having a slope 5% less than the initial compliance (C_0) crosses the force/extension curve. Energy (U) is calculated as the integral of the force/extension curve to the point of failure (i.e. the shaded area). Criterion for a valid CT test: $P_{max}/P_q \leq 1.10$. (B) The value of J was determined from the partial derivative of energy (U) by apparent crack length (a) for the extension (q) at which failure occurred. The solid line represents the regression of the data. The dashed line is a visual representation of J_{crit} for the sample which failed at the point designated a_{crit} .

Table 1. Tensile test results

| Orientation of load relative to tubules | N | Mean initial modulus | | Mean yield stress | |
|---|----|----------------------|-------|-------------------|------|
| | | (GPa) | s.d. | (MPa) | s.d. |
| Parallel | 19 | 0.410 | 0.032 | 9.18 | 0.42 |
| Perpendicular | 24 | 0.485 | 0.035 | 11.8 | 0.36 |

of plastic deformation. The J-integral is a measure of the instantaneous change in energy with an incremental change in crack length at the critical point of failure. It can be considered as the work required to extend a crack at the critical point of fracture. The evaluation of the critical J-integral value (J_{crit}) involved several steps. First, the energy (U) was plotted against the apparent crack length to specimen width ratio (a/W) for each interval of extension (Fig. 5B). Since crack length and specimen compliance are related, the magnitude of the energy value will also be related to crack length. At each extension level, then, J_{crit} was determined from the slope of this relationship [$U/(a/W)$] at the critical failure point (i.e. the extension at which $P = P_q$) for each of the individual specimens that failed at that extension. The slope was determined by taking the derivative of a polynomial regression of the U vs (a/W) data. The J-integral is defined by Broek (1978) as

$$J = (-1/B) \times (\partial U / \partial a)_q .$$

RESULTS

Tensile tests

The elastic modulus of a fibre-reinforced composite will depend on the relative angle of the individual fibres to the direction of applied stress, and on the proportion of fibres with a component of their orientation aligned with the direction of the stress (Wainwright *et al.* 1982). Although the obvious parallel arrangement of the tubules might suggest that the hoof-wall is strongly reinforced in the axial direction of the tubules, polarized light sections of the hoof-wall show a marked lateral orientation of fibres within the intertubular component. Because the tubular and intertubular components are present in roughly equal quantities, the resulting mix of fibre reinforcement may yield a material with nearly equal properties in both directions. The tensile tests indicate that this is indeed the case. The differences found between hoof-wall keratin tested either parallel or perpendicular to the tubular axes for initial modulus or yield stress (Table 1) are extremely small. This suggests that the intertubular material plays a more important role in determining the properties of the hoof than might be expected from viewing the more visually striking tubular morphology. This conclusion is confirmed in the fracture tests that follow.

Fracture tests

Compliance calibration of notch length

Fig. 6 shows the initial compliance (C_0) versus notch length ratio (A/W) for 62 samples cut in orientation 1, parallel to the tubular axis. The data extended over a

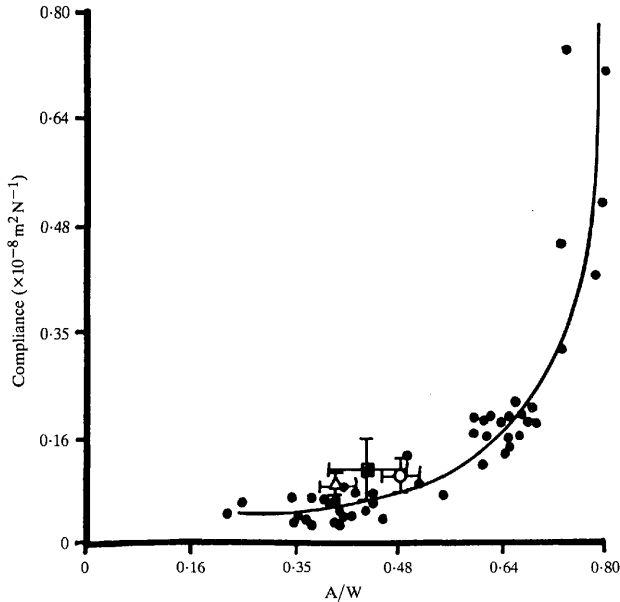


Fig. 6. Orientation 1 (solid dots) compliance calibration data used to determine apparent crack length. The regression was initially determined with compliance dependent on precut notch length (A) to specimen width (W) ratio ($r^2 = 0.88$; $N = 62$). The apparent crack length to width ratio (a/W) during a test for each specimen was determined from the measured mechanical compliance by reading the value predicted by the relationship between A/W and compliance. All orientations were applied to the same regression because the results of all orientations were similar, as described in the text. Initial compliance data for orientations 2–4 are indicated as mean value and standard deviation. Open circle, orientation 2; triangle, orientation 3; square, orientation 4.

wide range of A/W values and were best described by a third-order polynomial ($P < 0.001$; $r^2 = 0.88$). This compliance calibration relationship was also used to determine the crack lengths in the fracture studies of orientations 2–4 because all points from these other orientations fit the orientation 1 calibration curve well (see Fig. 6). This is not surprising because compliance is a measure of material stiffness and, as demonstrated above, specimen orientation does not greatly affect horse hoof keratin stiffness in tensile tests.

Fracture toughness

The data available for orientation 1, in which the notch was placed parallel to the tubules, represent the largest homogeneous group of samples. This data set was used to evaluate several features of the material which could have effects on the fracture toughness measurements of the hoof-wall. These features are (1) vertical location

Table 2. Fracture toughness in relation to vertical position

| Location | <i>N</i> | Mean J_{crit} ($\times 10^4 \text{ J m}^{-2}$) | s.d. |
|--------------|----------|---|------|
| 1 (proximal) | 3 | 0.98 | 0.22 |
| 2 | 10 | 1.20 | 0.15 |
| 3 | 7 | 1.35 | 0.25 |
| 4 | 10 | 1.13 | 0.11 |
| 5 (distal) | 5 | 0.52 | 0.08 |

within the hoof, (2) individual from which the sample was taken and (3) pigmentation of the sample. Pigmentation was determined by visual inspection as either being highly pigmented (i.e. black) or obviously unpigmented (i.e. white). Intermediate levels of pigmentation, which constitute a gradient between these two extremes, were excluded from this comparison. Analysis of variance and multiple comparison tests (Tukey's) indicate there is no statistical difference between the mean J_{crit} value for either pigmented and unpigmented samples or between different individuals.

A significant difference in fracture toughness was found for the most distal portion of the hoof-wall. The strips of hoof-wall from which test blocks were cut represent a vertical stack of samples. Approximately 1 cm was discarded from both the upper and lower ends of each strip and the remainder was divided into five sections which represented a proximal location at one end and a distal location at the other. The five vertical locations were then analysed for their fracture toughness. The mean J_{crit} value for the most distal location is significantly lower than in the other more proximal locations (Table 2). There are no significant differences between the four proximal locations; the mean J_{crit} for these locations was $1.19 \times 10^4 \text{ J m}^{-2}$. In the most distal location, however, the mean J_{crit} value falls by about half to $5.2 \times 10^3 \text{ J m}^{-2}$. The data from location 5 are significantly different from those at positions 2, 3 and 4 ($P < 0.05$). For this reason, data from this distal position are omitted from all further analyses. This observation is interesting because the distal location is the oldest tissue present in the wall. This suggests that the hoof-wall keratin accumulates fatigue damage with long-term impact loading that weakens the distal portions of the hoof. Fatigue damage for most composite materials is due to the formation of micro-cracks (Gordon, 1976).

Table 3 gives the results of fracture toughness tests on hoof-wall samples cut with notch orientations 1–4, as described in Materials and Methods (see Fig. 4). These data demonstrate the importance of the intertubular material with respect to fracture toughness of the hoof-wall. Orientation 1 shows the highest mean fracture toughness. The orientation of the notch in this case represents a crack that would run parallel to the tubules, in a proximal direction within the hoof. In this case the precut notch was oriented across the direction of the intertubular material at a mean angle of 58.9° . For orientation 3 the notch runs perpendicular to the tubular direction. If hoof-wall keratin is a composite in which the tubules act as reinforcing fibres and the intertubular portion merely as a matrix, then the fracture toughness of orientation 1

(fracture in the direction of the tubule axis) should be lower than that of orientation 3 (fracture across the grain of the tubules). This is obviously not the case (Table 3). Although there is no statistically significant difference between the data for orientations 1 and 3, the mean J_{crit} value for orientation 1 is somewhat higher than that for orientation 3. This suggests that the dominant feature of hoof-wall structure may be the intertubular material.

Comparison of the results for orientations 2 and 4 illustrates this more clearly. Recall that in these samples the notches were cut perpendicular (orientation 2) and parallel (orientation 4) to the intertubular direction. In both cases the notch runs at a similar angle to the tubular axis. This comparison, then, focuses on the role of the intertubular material orientation. The fracture toughness for orientation 4 (notch parallel to intertubular direction) is significantly lower ($P < 0.05$) than for orientation 2 by a factor of more than two (Table 3).

To verify that fracture in hoof-wall is dominated by the orientation of the notch relative to the intertubular direction, the direction of crack growth in each sample was subjected to linear regression analysis with respect to tubular and intertubular direction. No significant relationship was found between crack growth direction and tubular direction; whereas a significant relationship was found between the crack growth direction and intertubular direction (see Fig. 7).

A graphic demonstration of the dominance of the intertubular direction over crack growth is seen by inspection of the CT specimens after fracture (Fig. 8). Typical fracture paths observed for samples with orientations 2 and 4 show that, in spite of the fact that the CT test regime is designed to drive the crack parallel to the precut notch, the crack, as shown in Fig. 8A (precut notch perpendicular to intertubular orientation), has grown at right angles to the notch. Thus, the crack has been diverted from its original direction of growth by the intertubular material. When the intertubular direction is oriented parallel to the notch (Fig. 8B), the crack, as expected, grows in the direction of the original notch. This behaviour was seen for virtually all samples with orientations 2 and 4.

DISCUSSION

The fracture toughness of hoof-wall keratin

The selection of the most appropriate technique for measuring work of fracture depends on the type of material being tested. The compact tension test geometry has

Table 3. *Fracture toughness in relation to morphological organization*

| Orientation | N | Mean angle relative to notch (degrees) | | J_{crit} ($\times 10^4 \text{ J m}^{-2}$) | S.E. |
|-------------|----|--|--------------|--|------|
| | | Tubular | Intertubular | | |
| 1 | 30 | 0 | 58.9 | 1.19 | 0.09 |
| 2 | 8 | 39.3 | 75.5 | 0.80 | 0.14 |
| 3 | 9 | 90 | 35.2 | 1.08 | 0.11 |
| 4 | 6 | 43.8 | 14.1 | 0.46 | 0.05 |

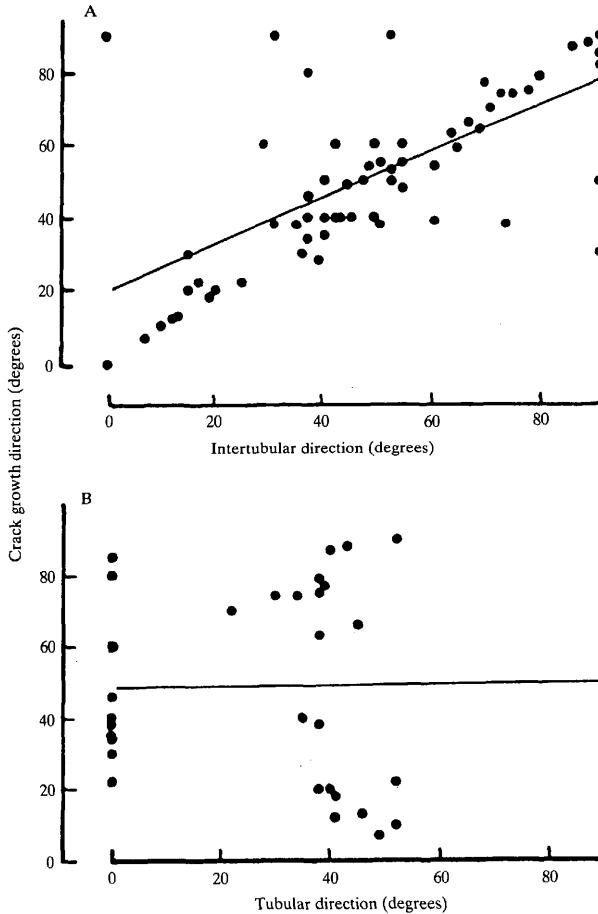


Fig. 7. (A) Linear regression analysis of intertubular material orientation *versus* crack growth direction (both relative to precut notch). $r = 0.68$; $N = 119$; $t = 10.02$; $P < 0.05$. (B) Linear regression analysis of tubular orientation *versus* crack growth direction (both relative to precut notch). Slope not significant.

been used successfully with stiff composite biomaterials such as bone (Wright & Hayes, 1977) and wood (DeBaise, Porter & Pentoney, 1966). In both of these studies linear elastic stress-strain behaviour was assumed over the course of the test, and fracture toughness was calculated with the strain energy release method of Irwin (1958). For bone and wood the assumption of linear elasticity may be reasonable, but

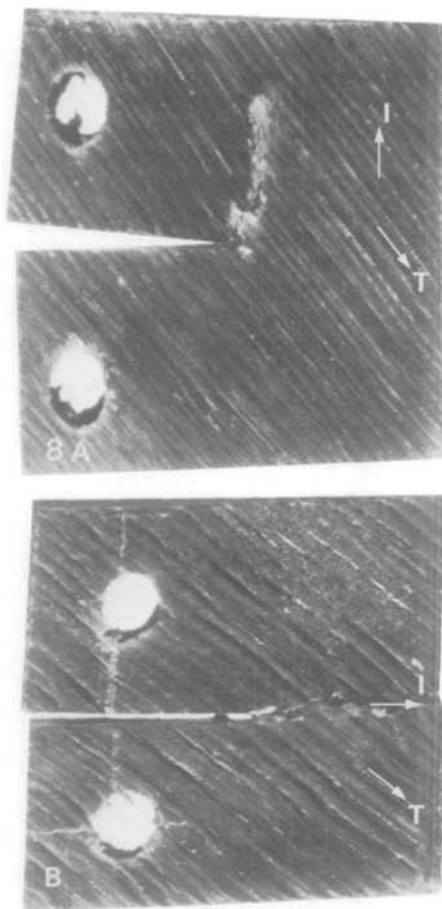


Fig. 8. The direction of crack propagation is seen to follow the intertubular material direction rather than the tubule direction. (A) A specimen with orientation 3 in which the precut notch is perpendicular to the intertubular direction (I). (B) A specimen with orientation 4 in which the intertubular direction is parallel to the precut notch. The region of crack growth can be clearly seen emanating from the tip of the notch. Note that the direction of the tubular material (T) is at approximately 45° to the precut notch in both cases.

the post-yield plastic deformation seen for hoof-wall keratin makes the method inappropriate in this case. We therefore used the J-integral analysis because it is designed to provide an accurate measure of the work of fracture for materials that exhibit significant elastic-plastic behaviour.

For brittle materials like glass, the work of fracture is quite close (approximately 6 J m^{-2}) to the true surface energy of the material (about 1 J m^{-2} for most materials; Gordon, 1976). For tough materials, however, a variety of mechanisms inhibit crack growth by dramatically elevating the energetic cost of creating fracture surfaces. Horse hoof keratin, for example, has a work of fracture of about $10\,000 \text{ J m}^{-2}$. Thus, keratin is some 2000 times tougher than glass, and it is clear why keratin is a more suitable structural material. Horse hoof keratin also compares quite well with other tough biomaterials. Fresh bone, for example, has a work of fracture of about $1000\text{--}3000 \text{ J m}^{-2}$ (Wright & Hayes, 1977) and wood has a work of fracture of about $10\,000 \text{ J m}^{-2}$ (Jeronimidis, 1976). Thus, keratin is as tough as or tougher than other components of the vertebrate skeleton and is amongst the toughest biomaterials known. In comparison with engineering materials, keratin is good but not exceptional. The toughness of glass fibre-reinforced composites is similar to that of keratin, but the very best, continuous-fibre composites can approach $100\,000 \text{ J m}^{-2}$ (Harris, 1980).

The fracture design of hoof-wall

Hoof-wall is a fibre-reinforced composite at the submicroscopic level. It also has higher levels of organization which have important effects on the mechanical properties of the tissue. For instance, the tensile stiffness of hoof-wall keratin, at 400 MPa , is significantly less than that of other hard keratins, such as hair and wool ($1.5\text{--}2.5 \text{ GPa}$; Fraser & MacRae, 1980). This difference is due in part to the complex structure of the hoof-wall, which contains roughly equal quantities of alternately oriented tubular and intertubular material. Hair and wool are tubular structures with all the microfibrils oriented roughly parallel to the axis of the strand, and the material behaves as a highly reinforced, parallel-fibre composite. In our tensile samples of hoof-wall keratin, either the tubular or intertubular material was oriented with its microfibre direction perpendicular to the applied load (i.e. as a series composite), and thus the reinforcement will be less in the hoof-wall material. This particular organization, however, produces a material with a more uniform response to loading in different directions (i.e. properties that are more isotropic).

The complex architecture of hoof-wall also has important consequences for the fracture behaviour. The correlation found between fracture toughness and the orientation of the intertubular material relative to the notch (Table 3) indicates that the fracture behaviour of hoof-wall keratin is dominated by the intertubular material. In addition, the strong correlation between the direction of crack growth and the intertubular orientation (Fig. 7) indicates that fracture virtually always occurs in the plane of the intertubular material. Because the microfibre orientation of the intertubular material in the intact hoof runs normal to the longitudinal axis of the hoof and parallel to the ground contact surface, the intertubular material prevents cracks

from progressing proximally in the hoof. In fact, because it was virtually impossible in our tests to propagate a crack across the intertubular direction, the fracture toughness values obtained for test orientations that attempted to propagate cracks parallel to the long axis of the tubules (orientation 1) or perpendicular to the intertubular orientation (orientation 2) must represent minimum estimates of the work of fracture for crack growth in the proximal direction in the hoof.

The intertubular material orientation obviously reinforces the wall against fracture in the proximal direction, but, if only keratin with this orientation were present, it would produce a plane of extreme fracture weakness in the lateral direction. This would occur because the microfibre orientation which limits proximally oriented fracture would not be present for laterally oriented fracture. Hoof-wall would then be expected to fracture easily in this plane, just as a block of wood can much more easily be split when chopped with the grain than against it. However, in hoof-wall the tubular material has an orientation which crosses that of the intertubular material. Because the intertubular orientation dominates the fracture behaviour so dramatically, it was not possible to isolate the effects of the tubular material in the same way as for the intertubular material. Our understanding of fracture behaviour in composites would predict, however, that the tubular material, with its perpendicular microfibre orientation, would resist fracture in the lateral direction by obstructing the growth of cracks parallel to the intertubular direction in much the same way as knots increase the energy necessary to split a block of wood, even when cutting with the grain.

Although hoof keratin possesses a very respectable fracture toughness, the least fracture-resistant direction remains the direction of the intertubular plane, in spite of the reinforcement by the tubular material. Indeed, in the fracture tests conducted, it was virtually impossible to cause a crack to grow across the grain of the intertubular material. Instead, the crack was diverted to the direction of the intertubular material, even when this direction was normal to the acute stress concentration applied in the CT samples (see Fig. 8). One would also expect this behaviour if an intense stress concentration occurred in the intact hoof as a result of the horse stepping on an uneven substrate. A crack produced by this situation would be diverted to the direction of the intertubular material even if it originally began to grow proximally. Because the hoof-wall keratin must grow from the proximal border to replace damaged wall, a proximally directed crack can cause severe, long-lasting damage. Thus, the intertubular material provides a 'safety valve', diverting potentially dangerous proximally directed cracks to a less dangerous lateral direction. It is interesting to note that, although there is some variation present, this plane of fracture weakness is oriented parallel to the ground contact surface (Fig. 9). The fore hooves of horses generally strike the ground at an angle of approximately 60° and the rear hooves at approximately 50° . This means that the tubules, which run parallel to the surface of the hoof-wall, must be oriented obliquely to the intertubular material in most of the hoof in order for the intertubular direction to be parallel to the distal contact surface. The mean tubular/intertubular angle in the samples used is about 56° (Table 1).

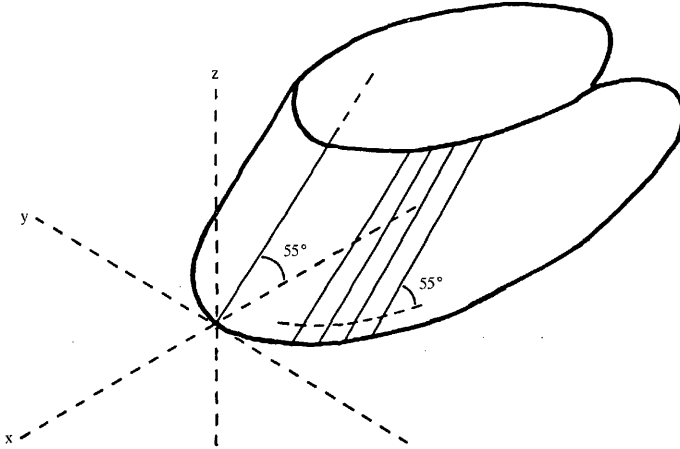


Fig. 9. Diagram showing the oblique relationship between the tubular axes (solid lines) and the plane of the intertubular material. The tubules run parallel to one another and strike the ground at an angle equivalent to that at which the wall strikes the ground (approx. 55°). The intertubular material runs parallel to the ground contact surface; therefore, it must be related to the tubular material at an oblique angle anywhere in the hoof-wall except at the centre toe.

Thus, the morphological organization produces a material with toughness properties which allow wear in a specific direction, the direction least detrimental to the animal.

The wear properties of hoof could actually assist in reducing the chance of fracture of the wall. The reduced fracture toughness of the distal portion of the wall (Table 2) indicates that the oldest tissue is subject to fatigue damage, most probably in the form of microcracks. Since fracture is more likely to spread from stress concentrations around flaws, such as microcracks, the controlled elimination of the damaged portion may reduce the likelihood of major cracks occurring.

Fibre orientation is a fundamental determinant of most mechanical properties in fibre-reinforced composites. As seen in hoof-wall intertubular material, planar fibre organization produces a material which is very anisotropic with respect to fracture toughness. In this case, the plane of weakness is reinforced by the tubular material which has fibres oriented to inhibit crack growth in the weak plane. Keratinocytes are only produced parallel to the basal epidermal membrane. In order for fibres to be oriented to resist fracture in the intertubular direction it is necessary for the arrangement of the basal epidermal membrane to be modified in a manner that produces cells oriented perpendicular to the intertubular material. Through the simple outpouching of the basal membrane to form the dermal papillae on which the tubules grow, the 'growth plane' of the tubule cells becomes oriented perpendicular to the intertubular material. As a result, a material possessing reasonable fracture stability in all three directions is created.

Mammals have developed an amazing diversity of hard keratin appendages. These take on an extremely wide variety of forms to accomplish an equally wide range of functions. Among these are hooves, claws, horns of various types and the baleen of whales. An interesting feature of all these structures is the presence of regions of tubular organization embedded in intertubular material (George, 1956; Earland, Blakey & Still, 1962; Ryder, 1962). Considering the results of this study, it is probable that the structural organization found in these tissues has an important influence on fracture toughness. The diverse variety of hard keratin appendages suggests that this structural organization could represent a fundamental response of epidermal tissues to functional roles which require materials with good fracture toughness and abrasion-resistant properties. It is a simple modification of the epidermal pattern which may provide significant advantages in these other tissues as it does in the horse hoof-wall.

We wish to thank Dr R. J. Gray, Faculty of Applied Science, University of British Columbia, for advice in designing this project. This manuscript has been improved by suggestions kindly provided by Dr M. LaBarbera, Dr L. Radinsky, Peter C. Wainwright and Karen O. O'Connor.

REFERENCES

- ASTM Standard E-399-80 Test for Plane Strain Fracture Toughness of Metallic Materials; *Annual Book of ASTM Standards*, part 10.
- BROEK, D. (1978). *Elementary Engineering Fracture Mechanics*. The Netherlands: Sijthoff & Noordhoff International Publishers.
- DEBAISE, G. R., PORTER, A. W. & PENTONEY, R. E. (1966). Morphology and mechanics of wood fracture. *Materials Research and Standards* **6**, 493-499.
- DINGER, J. E., GOODWIN, E. E. & LEFFEL, E. C. (1973). Factors affecting hardness of the equine hoof wall. Scientific paper No. A2212, Cont. No. 5193, Maryland Experimental Station, University of Maryland, 20742, USA.
- EARLAND, C., BLAKEY, P. R. & STILL, J. P. (1962). Molecular orientation of some keratins. *Nature, Lond.* **196**, 1287-1291.
- FRASER, R. D. B. & MACRAE, T. P. (1980). Molecular structure and mechanical properties of keratins. In *The Mechanical Properties of Biological Materials* (ed. J. F. V. Vincent & J. D. Currey). *Symp. Soc. exp. Biol.* **XXXIV**, 37-74.
- GAGGAR, S. & BROUTMAN, L. (1975). Crack growth resistance of random fibre composites. *J. comp. Mat.* **9**, 216-227.
- GEARY, J. E. JR (1975). The dynamics of the equine foreleg. MMAE thesis, University of Delaware.
- GEORGE, A. N. (1956). The post-natal development of the horn tubules and fibres in the horns of sheep. *Br. vet. J.* **112**, 30-34.
- GORDON, J. E. (1976). *The New Science of Strong Materials*. England: Penguin Books Ltd.
- HARRIS, B. (1980). The mechanical behaviour of composite materials. In *The Mechanical Properties of Biological Materials* (ed. J. F. V. Vincent & J. D. Currey). *Symp. Soc. exp. Biol.* **XXXIV**, 211-246.
- IRWIN, G. R. (1958). Fracture. In *Encyclopedia of Physics*, vol. 6 (ed. S. Flugge), pp. 551-590. Berlin: Springer-Verlag.
- JERONIMIDIS, G. (1976). The fracture of wood in relation to its structure. In *Wood Structure in Biological and Technological Research* (ed. P. Baas, A. J. Bolton & D. M. Catling). Leiden Botanical Series No. 3, pp. 253-265. Leiden: The University Press.

- LANDES, J. D. & BEGLEY, J. A. (1972). The effect of specimen size and geometry on J. *ASTM STP* **514**, 24.
- LEACH, D. H. (1980). The structure and function of equine hoof wall. Ph.D. thesis, Department of Veterinary Anatomy, University of Saskatoon, Saskatoon, Saskatchewan, Canada.
- NICKEL, R. (1938). Über den Bau der Hufrohren und seine Bedeutung für den Mechanismus des Pferdehufes. *Dt.-öst. tierärztl. Wschr.* **46**, 449–552.
- PARKER, R. A. (1973). The analysis of the forces and displacements in the digit of the horse during walk. M.Sc. thesis, Cornell University, Ithaca, NY.
- RICE, J. R. (1968). A path independent integral and the approximate analysis of strain concentration by notches and cracks. *J. appl. Mech.* **35**, 379.
- RYDER, M. L. (1962). Structure of rhinoceros horn. *Nature, Lond.* **193**, 1199–1201.
- SACK, W. O. & HABEL, R. E. (1977). *Rooney's Guide to the Dissection of the Horse*. Ithaca, NY: Veterinary Textbooks.
- WAINWRIGHT, S. A., BIGGS, W. D., CURREY, J. D. & GOSLINE, J. M. (1982). *Mechanical Design in Organisms*. Princeton, NJ: Princeton University Press.
- WILKENS, H. (1964). Zur makroskopischen und mikroskopischen Morphologie der Rinderklaue mit einem Vergleich der Architektur von Klauen- und Hufrohren. *Zentbl. vet. Med.* **11A**, 163–234.
- WRIGHT, T. M. & HAYES, W. C. (1977). Fracture mechanics parameters for compact bone – Effects of density and specimen thickness. *J. Biomech.* **10**, 410–430.